New Phytologist

The tomato plastidic fructokinase *SlFRK3* plays a role in xylem development

Ofer Stein[1,2], Hila Damari-Weissler[1], Francesca Secchi[3], Shimon Rachamilevitch[4], Marcelo A. German[1], Yelena Yeselson[1], Rachel Amir[5], Arthur Schaffer[1], N. Michele Holbrook[6], Roni Aloni[7], Maciej A. Zwieniecki[3] and David Granot[1]

[1]Institute of Plant Sciences, Agricultural Research Organization, The Volcani Center, Bet Dagan 50250, Israel; [2]The Institute of Plant Sciences and Genetics in Agriculture, The Robert H. Smith Faculty of Agriculture, Food and Environment, The Hebrew University of Jerusalem, Rehovot 76100, Israel; [3]Department of Plant Sciences, University of California, Davis, CA 95616, USA; [4]Albert Katz Department of Dryland Biotechnologies, Blaustein Institutes for Desert Research, Ben Gurion University, Sede Boqer Campus, 84990, Israel; [5]Laboratory of Plant Science, Migal Galilee Research Center, PO Box 831, Kiryat Shmona 12100, Israel; [6]Department of Organismic and Evolutionary Biology, Harvard University, 16 Divinity Ave., Cambridge, MA 02138, USA; [7]Department of Molecular Biology and Ecology of Plants, Tel Aviv University, Tel Aviv 69978, Israel

Author for correspondence:
David Granot
Tel: +972 3 9683792
Email: granot@agri.gov.il

Received: *6 August 2015*
Accepted: *8 September 2015*

New Phytologist (2016) **209:** 1484–1495
doi: 10.1111/nph.13705

Key words: fructokinase, fructose, plastid, RNAi, sucrose, tomato (*Solanum lycopersicon*), xylem fiber, xylem vessel.

Summary

- Plants have two kinds of fructokinases (FRKs) that catalyze the key step of fructose phosphorylation, cytosolic and plastidic. The major cytosolic tomato FRK, *SlFRK2*, is essential for the development of xylem vessels.
- In order to study the role of *SlFRK3*, which encodes the only plastidic FRK, we generated transgenic tomato (*Solanum lycopersicon*) plants with RNAi suppression of *SlFRK3* as well as plants expressing beta-glucoronidase (GUS) under the *SlFRK3* promoter.
- GUS staining indicated *SlFRK3* expression in vascular tissues of the leaves and stems, including cambium, differentiating xylem, young xylem fibers and phloem companion cells. Suppression of *SlFRK3* reduced the stem xylem area, stem and root water conductance, and whole-plant transpiration, with minor effects on plant development. However, suppression of *SlFRK3* accompanied by partial suppression of *SlFRK2* induced significant growth-inhibition effects, including the wilting of mature leaves. Grafting experiments revealed that these growth effects are imposed primarily by the leaves, whose petioles had unlignified, thin-walled xylem fibers with collapsed parenchyma cells around the vessels. A cross between the *SlFRK2*-antisense and *SlFRK3*-RNAi lines exhibited similar wilting and anatomical effects, confirming that these effects are the result of the combined suppression of *SlFRK3* and *SlFRK2*.
- These results demonstrate a role of the plastidic *SlFRK3* in xylem development and hydraulic conductance.

Introduction

Sucrose, a disaccharide, is an important end product of photosynthesis and the main sugar transported in the vascular systems of many plants, including tomato. Sucrose must be cleaved by either sucrose synthase (SUS), into UDP-glucose and fructose, or by invertase into glucose and fructose, in order to be further metabolized (Dennis & Blakeley, 2000). The free fructose and glucose must then be phosphorylated by fructokinase (FRK) or hexokinase (HXK) before it can be metabolized any further. FRK and HXK are distinguished by their substrate specificities and affinities (Renz & Stitt, 1993). FRK phosphorylates only fructose; whereas HXK phosphorylates both glucose and fructose. However, the affinity of HXK for fructose is two orders of magnitude lower than its affinity for glucose, as well as two orders of magnitude lower than the affinity of FRK for fructose. It is, therefore, likely that fructose is phosphorylated primarily by FRK (Granot, 2007).

Four different FRK-encoding genes, known as *SlFRK1-4*, have been isolated from tomato (*Solanum lycopersicon*) plants (Kanayama *et al.*, 1997, 1998; German *et al.*, 2002, 2004; Granot, 2007). *SlFRK4* is expressed only in stamens and pollen, whereas the other three *SlFRK* genes are expressed in all plant parts that have been examined (German *et al.*, 2002, 2003, 2004). Yet, *SlFRK2* and *SlFRK3* are the major FRK genes expressed in most plant parts (German *et al.*, 2004). The enzymes encoded by each FRK gene have unique localization and biochemical properties. SlFRK1, SlFRK2 and SlFRK4 isozymes are found in the cytosol, whereas SlFRK3 is found in the stroma of plastids (Damari-Weissler *et al.*, 2006). In addition, unlike the SlFRK1 and SlFRK4 enzymes, the fructose-phosphorylation activity of SlFRK2 and SlFRK3 is inhibited by fructose concentrations above 1 mM – a phenomenon known as substrate inhibition (Petreikov *et al.*, 2001; German *et al.*, 2004).

It has been proposed that FRKs might play a key role in starch synthesis because the starch-accumulation phase of young tomato fruits is characterized by the increased activity of FRK and SUS, as well as the increased activity of two key enzymes in starch biosynthesis, ADP-glucose pyrophosphorylase and starch synthase (Schaffer & Petreikov, 1997). However, a more recent study found that suppression of *SlFRK2* increased starch concentrations in young tomato fruits, indicating that *SlFRK2* is not required for the accumulation of starch (Dai *et al.*, 2002). Rather, it has been shown that *SlFRK2* is essential for proper xylem and phloem development (Damari-Weissler *et al.*, 2009). The xylem vessels in stems of *SlFRK2*-antisense plants have thinner secondary cell walls and are narrower and deformed, and the sieve elements are smaller. As a result, sugar transport and water conductance are reduced, causing severe growth inhibition and the wilting of young leaves (Damari-Weissler *et al.*, 2009).

Although *SlFRK2* is required for vascular development, the roles of the other FRKs are not known. The different expression patterns and biochemical characteristics of the different FRK genes might suggest that each of these genes plays a specific and unique role (German *et al.*, 2004; Damari-Weissler *et al.*, 2009). Because *SlFRK3* is the second most abundant fructose-phosphorylating enzyme (German *et al.*, 2004) and the only plastidic FRK in tomato (Damari-Weissler *et al.*, 2006), we decided to conduct a functional analysis of its role *in planta*.

Materials and Methods

Plant material

Tomato (*Solanum lycopersicon* (L.) H. Karst.) plants of cultivar MP1 (Barg *et al.*, 1997) were used to generate all of the transgenic lines. The DNA of the BAC-292L05 was used for PCR amplification of the *SlFRK3* promoter region. A 1855-bp fragment of the *SlFRK3* promoter was amplified with a pair of primers carrying *Sal*I and *Sma*I restriction sites (Supporting Information Table S1). After digestion, the DNA fragment was inserted into the pGPTV plant binary vector, which had been predigested with *Sal*I and *Sma*I. pGPTV includes a *GUS* reporter gene and the neomycin phosphotransferase II (*NptII*) gene as a selectable marker.

An 880-bp fragment of tomato fructokinases 3 (*SlFRK3*) (Fig. S1) was amplified using the primers listed in Table S1 and introduced in RNAi orientation under the control of the cauliflower mosaic virus 35 promoter into the binary vector pGREEN containing the neomycin phosphotransferase II gene (*nptII*) as a selectable marker. T_0 independent transgenic plants were analyzed by PCR for the presence the *npt*II gene. Homozygous plants were identified among T_1 seeds following kanamycin-resistant segregation analysis of *npt*II and their relative expression of *SlFRK3* was examined using real-time PCR. Three independent lines exhibiting suppression of *SlFRK3* were identified (F3R1, F3R3 and F3R4).

Histochemical localization of GUS activity

In order to localize the beta-glucoronidase (GUS) activity, leaves, stems and petioles of the transgenic plants were infiltrated with 1 mM 5-bromo-4-chloro-3-indolyl-glucuronide (X-Gluc) in 50 mM sodium phosphate buffer pH 7 containing 0.5 mM $K_3Fe(SCN)_6$, 0.5 mM $K_4Fe(SCN)_6$ and 1 mM EDTA and incubated overnight at 37°C. After incubation, the plant material was cleared with 70% ethanol and the leaves were photographed. Freehand cross-sections were made from petioles and stems to visualize GUS staining at the cellular level. These cross-sections were rinsed in water and examined under transmitted white light.

RNA extraction and cDNA generation

Tissue samples from tomato plants were frozen and homogenized in liquid nitrogen. RNA was extracted using the EZ-RNA kit (Biological Industries, Kibbutz Bet Haemek, Israel), with up to 500 µl of frozen homogenized tissue per extraction tube. Two to three independent extractions were performed for each tissue set. The extractions were carried out according to the manufacturer's instructions. RNA pellets were suspended in 25 µl DEPC-treated H_2O and treated with DNase (Ambion) according to the manufacturer's instructions. The presence of RNA was confirmed by gel electrophoresis and DNA degradation was confirmed by PCR. RNA ($\leq$ 1 µg) from each sample was reverse-transcribed to cDNA using MMLV RT (Promega) in a 25-µl reaction, with 2 µl of random primers and 1 µl of mixed poly-dT primers (18–23 nt), for the generation of cDNA from both rRNA and mRNA. All cDNA samples were diluted 1 : 8 in water.

Real-time expression analysis

Real-time reactions were prepared with SYBR Green mix (Eurogentec S.A., Seraing, Belgium) in 10-µl aliquots with 4 µl diluted cDNA per reaction, two replicates per cDNA sample. Reactions were run in a RotorGene 6000 cycler (Corbett, Mortlake, NSW, Australia), 40 cycles per run, with sampling after each cycle. Results were interpreted with RotorGene software, with normalization for each tissue set (three independent samples, two duplicates per sample). Cyclophilin was used as a reference gene for normalization. The specificity of the primers for each gene was confirmed by testing them with DNA plasmids containing the other FRK genes. Unique peaks were observed for each FRK gene and these peaks were in complete agreement with those of their respective DNA controls. The primers used for the quantitative real-time PCR analysis are listed in Table S1.

Effect of VPD on whole-plant transpiration

Plants were grown in a glasshouse in 5-l pots until they had developed 12–14 fully expanded leaves. The transpiration-rate response to vapor pressure deficit (VPD) was measured in the laboratory by placing the plant shoot in a chamber in which VPD can be manipulated (Sinclair *et al.*, 2008). A box fan was placed inside the shoot chamber to rapidly stir the air and

minimize boundary layer conductance and its impact on plant water loss rate. Absolute humidity in the shoot chamber was adjusted by changing the rate of airflow (15–45 l min^{-1}) through the shoot chamber and the humidity of the air. The plant shoot was exposed to 800 μmol m^{-2} s^{-1} photosynthetically active radiation and kept at a temperature of 26 ± 1°C. Air temperature and leaf temperature were measured and rarely differed by > 0.3°C. Air VPD was calculated based on the measured air temperature and the relative humidity in the chamber. A balance was placed under the pot to measure changes in plant weight. As the plant stem was not sealed in the shoot chamber, the stem could move freely in a slot within the chamber without affecting the measurement of plant weight. Weight was recorded every 30 s. Once a new level of humidity was established in the chamber, a new steady transpiration rate was usually reached within *c.* 20 min. The transpiration rate was calculated by linear regression during the steady-state period from the decrease in pot weight over 20 min. Data were collected from at least five plants of each genotype. The transpiration rates for individual plants and treatments were plotted against the VPD to which the plant shoots were exposed.

Hydroponic treatment

Seeds were planted on wet filter paper (Whatman Quantitative Circles, 90 mm, cat. no. 1001 090, Whatman®; Schleicher & Schuell, Dassel, Germany) in covered Petri dishes and left to germinate in darkness at room temperature. Three days after germination, the seedlings were moved to aerated hydroponic culture in 6.5-l containers filled with modified Hoagland solution (*c.* pH 6.1; 795 μM KNO_3, 603 μM $Ca(NO_3)_2$, 270 μM $MgSO_4$ and 109 μM KH_2PO_4; micronutrients: 40.5 μM Fe(III)-EDTA, 20 μM H_3BO_4, 2 μM $MnSO_4$, 0.085 μM $ZnSO_4$, 0.15 μM $CuSO_4$ and 0.25 μM Na_2MoO_4) and maintained in a growth chamber (PAR 600 mM; temperature: 25°C day and 21°C night; 65% humidity). After 1 wk, the young plants were transferred to 42-l boxes (12 plants per box) and the culture media was replaced twice a week.

Forced root exudation

The hydraulic conductance of tomato root systems was determined by measuring the flow induced in response to an applied pressure gradient (Gorska *et al.*, 2008). De-topped root systems were fitted with a plastic tube filled with DI water and connected to a beaker located on a balance (± 0.01 mg). The root system was sealed in a chamber containing the hydroponic solution in which the plants had been grown. The pH of the solution was kept at *c.* 6.1 using MES (2-(*N*-morpholino) ethanesulfonic acid) buffer (1 g l^{-1}). The pressure in the chamber was regulated using a needle valve, which was adjusted to allow a small leak in the chamber, such that air used to pressurize the chamber also served to aerate the medium. Water flow through the root system was automatically recorded by a computer at 30-s intervals. Flow stabilization occurred 10–20 min after the plant was exposed to pressure. Flow data were then collected for a 60-min period. At the end of each experiment, the fresh weights of the roots and shoots were recorded. The shoots and roots were then dried in an oven for 72 h at 90°C, after which the dry weights of these tissues were recorded and the root: shoot ratio was calculated (Gorska *et al.*, 2008).

Stem hydraulic conductivity

Stem hydraulic conductivity (K_h) was assessed on 5–10 main stems of plants of each genotype using stem pieces 5–10 cm in length. (A preliminary assessment showed that segment length did not affect K_h, as long as each segment was at least 5 cm long.) Deionized, degassed and filtered (0.2-μm filters) water was used as a perfusion solution. Stems were first perfused under elevated pressure (150 kPa) to remove any embolisms and hydraulic conductivity was then calculated as the pressure difference across the stem divided by the volumetric flow and stem length. Xylem cross-sectional area was microscopically determined for each stem to allow the calculation of the xylem-specific conductivity (K_s, which equals K_h divided by total xylem area). Leaf area distal to each measured stem was determined with an area meter (LI-3100; Li-Cor, Lincoln, NE, USA), which allowed us to calculate the leaf-specific conductivity (K_L; K_h divided by leaf area) to be determined (Kocacinar & Sage, 2004).

Leaf hydraulics as measured by rehydration

Whole stems were detached from glasshouse-grown plants and allowed to dry briefly on a laboratory bench to a leaf water potential of −0.3 to −0.7 MPa. After this brief drying, a stem segment associated with a single leaf was placed in a guillotine-like apparatus that allowed us to sever the petiole from the stem segment under water and connect the cut petiole to a water reservoir in a single step (Zwieniecki *et al.*, 2007). The water reservoir was placed on a high-resolution balance (± 10 μg) and the amount of water taken up by the rehydrating leaf was recorded every second. During this rehydration, the submerged leaf was exposed to *c.* 800 μmol m^{-2} s^{-1} photosynthetically active radiation. Preliminary measurements showed that submerging the lamina did not alter leaf water potential, indicating that any uptake of water through the leaf surface did not influence the measurement. Water-uptake kinetics were analyzed assuming a two-compartment, exponential model (Zwieniecki *et al.*, 2007). Time constants for rehydration and hydraulic conductance were calculated for the fast-uptake compartment, which was assumed to be indicative of water flow in the epidermal compartment of the leaves. A total of eight plants of each genotype were measured. We examined one leaf from each of these plants.

Anatomical techniques

For studying and analyzing the anatomy of both the phloem and the xylem tissues, freehand cross-sections were taken from the center of various internodes and leaf petiole along the shoots of the transgenic *SlFRK3*-RNAi lines that were compared to wild-type (WT) plants. The cross-sections were stained for a few seconds in 2% lacmoid (Polyscience, Warrington, PA, USA) in

96% ethanol, then rinsed in tap water for a few minutes, mounted in 50% sodium lactate (Aloni, 1980) and observed under transmitted white light. The lacmoid stains lignin in the cell walls of xylem vessels and fibers marine blue (Figs 9, 11).

The plant material shown in Fig. S2 was fixed in FAA (formalin, acetic acid), a mixture of 5% glacial acetic acid, 3.7% formalin, 50% ethanol and 41.3% water, and embedded in paraffin. Paraffin sections (10–20-μm thick) were stained with Safranin-O and Fast Green.

Freehand cross-sections (Fig. S3) were also taken from the petiole and leaf–petiole junction of both the F3R4 and the Wt plants. The cross-sections were rinsed in tap water for a few minutes and then examined under transmitted white light.

Sugar assays

Sugars were extracted from stem segments by resuspending the segments in 5 ml of 80% ethanol in an 80°C water bath for 60 min. This procedure was repeated twice. The ethanol solutions were combined and completely evaporated at 40°C with the aid of continuous ventilation. The dried sugars were dissolved in 1 ml distilled water and were stored frozen (−80°C) until they could be analyzed. Sucrose, fructose and glucose contents were determined by HPLC. The HPLC system consisted of a Shimadzu LC10AT solvent delivery system and the sugar was detected using a Shimadzu RID10A refractive index detector. Separation was carried out on an Alltech 700 CH Carbohydrate Column (Alltech, Deerfield, IL, USA) maintained at 90°C with a flow rate of 0.5 ml min^{-1}, according to the manufacturer's recommendations. The ethanol-insoluble residue was used to determine the starch concentration. Starch digestion was carried out by incubating and autoclaving samples with 6 ml water, and then adding 4 ml of buffer containing 200 units of amyloglucosidase and incubating overnight at 55°C (Dinar *et al.*, 1983). The amount of released glucose was determined using Sumner reagent. Optical density was determined at 550 nm.

Results

The *SlFRK3* promoter drives expression in the vascular tissues of leaves, petioles and stems

In order to determine in which tissues *SlFRK3* is expressed, we isolated a 1.855-kb section of the *SlFRK3* promoter region including the 233 bp 5′ UTR, fused it to the GUS reporter gene and used it to generate two independent transgenic tomato plants. GUS staining of $SlFRK3_{promoter}$*::GUS* plants showed expression in vascular tissues in stem and leaves. Examination of cross-sections of stems and leaf petioles revealed specific expression in the cambium and differentiating xylem, young xylem fibers and phloem companion cells (Fig. 1).

Generation and expression analysis of transgenic tomato plants in which *SlFRK3* was suppressed

In order to study the role of *SlFRK3 in planta*, we generated transgenic tomato plants with RNAi suppression of *SlFRK3* expressed under the 35S promoter. Three independent transgenic tomato lines with almost complete suppression of *SlFRK3* in their leaves, stems and petioles were obtained and are referred to as F3R1, F3R3 and F3R4 (Fig. 2). Because the 880-bp RNAi fragment of tomato *SlFRK3* shares significant levels of sequence identity with the corresponding regions of *SlFRK1* and *SlFRK2* (63.4% and 59.6%, respectively; Fig. S1), we examined the effects of *SlFRK3*-RNAi on the levels of *SlFRK1* and *SlFRK2* mRNA. F3R1 lines exhibited specific and significant suppression of *SlFRK3* (Fig. 2). The F3R3 plants exhibited significant suppression of *SlFRK3*, as well as significant suppression of *SlFRK1* in their leaves (73%), stems (60%) and petioles (82%). We also observed significant suppression of *SlFRK2* in leaves (43%) and petioles (81%), but not in stems (Fig. 2). The F3R4 plants exhibited suppression of *SlFRK3* and *SlFRK1*, much like we observed in the F3R3 plants, and also exhibited significantly greater

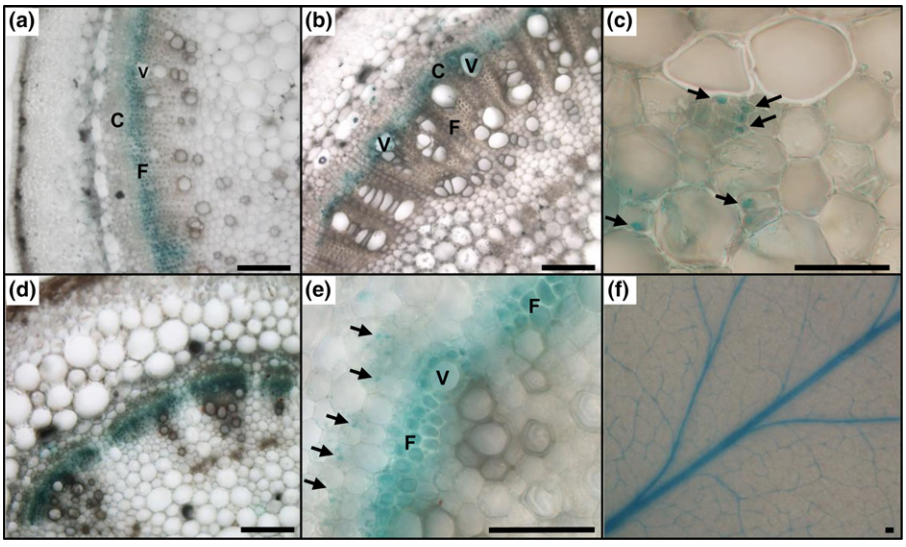

Fig. 1 The *SlFRK3* promoter is expressed in tomato (*Solanum lycopersicon*) vascular tissues. Histochemical analysis of the expression of the *SlFRK3* promoter in tomato tissues, as visualized by beta-glucoronidase staining. (a) Cross-section of stem internode no. 4 from the top (as numbered in Goren *et al.*, 2011) (b) Cross-section of stem internode no. 7 (from the top). (c) Enlargement of cross-section of stem internode no. 4 (from the top) that shows staining of phloem companion cells. (d, e) Cross-section of the petiole of leaf no. 3. (f) Leaf blade of a leaflet from leaf no. 5. C, cambium; F, xylem fibers; V, vessel; arrows, phloem companion cells. Bars: (a, b, d–f) 200 μm; (c) 50 μm.

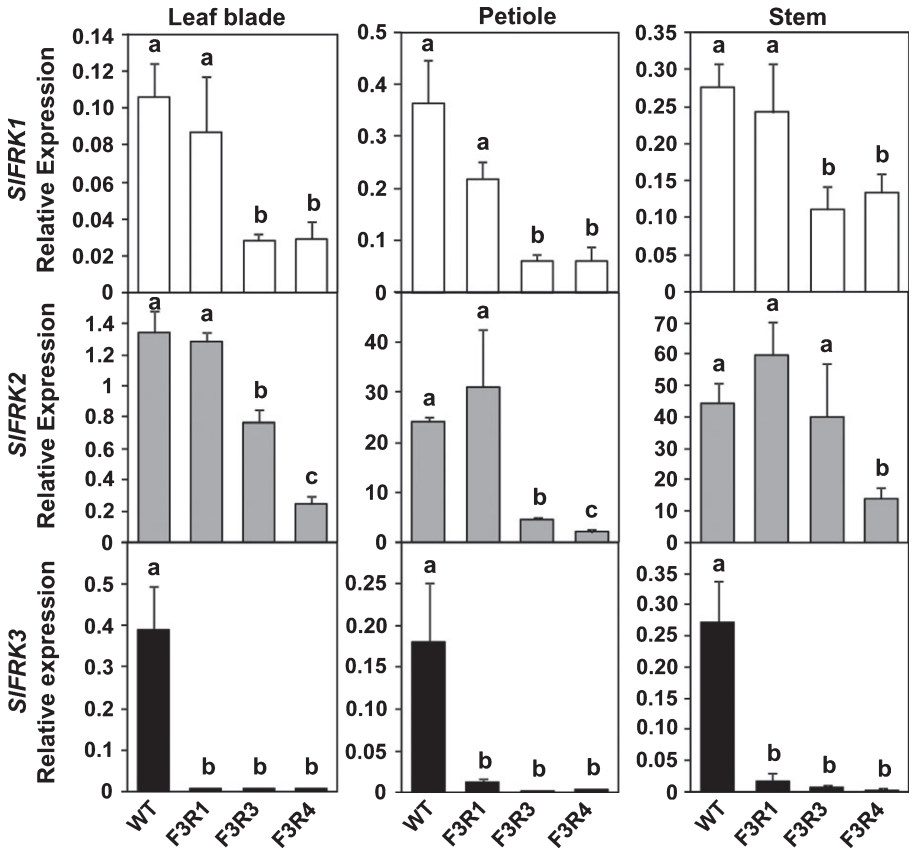

Fig. 2 Expression of *SlFRK* genes in the leaf blade, petioles and stems of *SlFRK3*-RNAi tomato (*Solanum lycopersicon*) plants. Samples were taken from leaf no. 6 and from stem internode no. 6 (from the top). Relative expression of three *SlFRK* genes in the different tomato lines and tissues was determined by real-time expression analysis with gene-specific primers (Supporting Information Table S2). Expression was normalized to the expression of cyclophylin in each sample. Data points represent means (± SE) of three plants. Different letters represent a statistically significant difference (Student's *t*-test; $P < 0.05$). WT, wild-type.

suppression of *SlFRK2* not only in their leaves (82%) and petioles (92%), but also in their stems (69%; Fig. 2).

F3R4 plants exhibited the wilting of mature leaves, thin stems, reduced biomass and increased flower abortion

Although the F3R1 and F3R3 lines exhibited no visibly unusual growth phenotypes (Fig. 3a), F3R4 plants had thinner stems (Fig. 3c) and their mature leaves wilted (Fig. 3a). Flower numbers for the transgenic lines were similar to that of the control plants, but the *SlFRK3*-RNAi lines exhibited significant loss (abortion) of flowers (Fig. 3b,d). The rates of flower abortion for F3R1, F3R3 and F3R4 were 22%, 28% and 89%, respectively, as compared with only 8% among the wild-type (WT) plants (Fig. 3d).

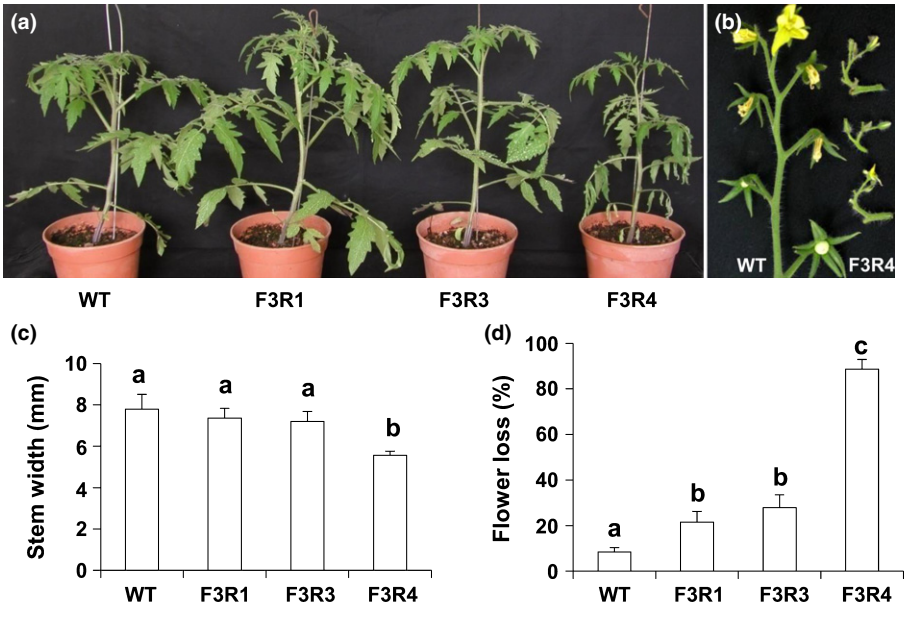

Fig. 3 Phenotypes of *SlFRK3*-RNAi transgenic tomato (*Solanum lycopersicon*) plants. (a) *SlFRK3*-RNAi transgenic tomato plants 7 wk after germination (WT, wild-type). (b) WT (left) and F3R4 (right) inflorescences. F3R4 inflorescences showed a high degree of flower loss. (c) Stem width of *SlFRK3*-RNAi transgenic tomato plants 7 wk after germination. Data represent means (± SD) of at least five plants ($n \geq 5$). Different letters represent values that are significantly different (Student's *t*-test; $P < 0.05$) (d) Flower loss of *SlFRK3*-RNAi transgenic tomato plants. Flower loss was determined based on the first four inflorescences of 4-month-old plants. Data points represent means (± SE) of at least six plants ($n \geq 6$). Different letters represent values that are significantly different (Student's *t*-test; $P < 0.05$).

Suppression of *SlFRK3*-reduced transpiration

The wilting phenotype observed in the mature leaves of the F3R4 lines indicated potential interference in the plants' water balance, suggesting that either water loss increased or water uptake and transport were reduced. To examine whether the suppression of *SlFRK3* had an effect on water loss, we followed whole-plant transpiration rates at different VPD levels and compared these rates to those of WT plants. All three lines showed reduced rates of transpiration (Fig. 4), eliminating the possibility that the observed leaf wilting might have been the result of increased water loss. Furthermore, whereas F3R1 and F3R3 lines showed reduced transpiration only under high VPD conditions (Fig. 4a), the wilting line (F3R4) showed greater reduction in its rate of transpiration than F3R1 and F3R3 even under very humid conditions (low VPD; Fig. 4b). This observation supports the notion that *SlFRK3* suppression affects water uptake or transport rather than water loss. The stomatal apertures of the three lines were significantly smaller than those of the WT plants (Table S2), also indicating that the observed wilting is not the result of increased water loss, but rather is due to reduced water uptake and/or transport.

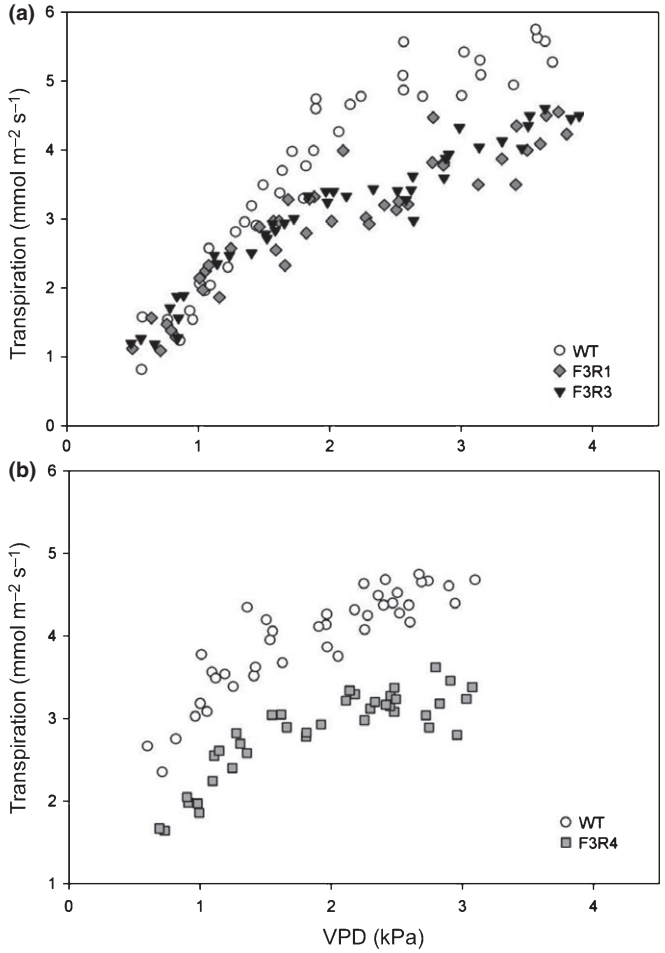

Fig. 4 *SlFRK3* suppression reduces transpiration. Whole-plant transpiration of *SlFRK3*-RNAi transgenic tomato (*Solanum lycopersicon*) plants (F3R1, F3R3 and F3R4) plotted against atmospheric vapor pressure difference (VPD), compared to the transpiration of wild-type (WT). The transpiration rates were calculated on a leaf-area basis for each individual plant ($n \geq 5$).

Suppression of *SlFRK3* led to reduced water conductance in stem and roots

Water conductance was measured in the roots, stem and leaves of the three transgenic lines. Stem hydraulic conductance in those three lines was lower than that of the WT. The levels of hydraulic conductance normalized to leaf area (K_L) of F3R1 and F3R4 were 20% and 75% lower than that of the WT, respectively (Fig. 5a,b). The K_L of F3R3 was also reduced by *c.* 15%, but this reduction was not statistically significant (Fig. 5a). When hydraulic conductivity was normalized to xylem area (K_s), statistically significant reductions of 40%, 20% and 80% were observed for F3R1, F3R3 and F3R4, respectively (Fig. 5c,d).

F3R1 exhibited reduced relative stem xylem area, but no significant reduction in stem xylem area was observed in the F3R3 or F3R4 plants (Fig. S2a,b). However, the F3R4 plants had thin stems and fewer xylem vessels than the WT plants (Fig. S2c,d). This suggests that the reduction of water transport in the stems of *SlFRK3*-RNAi lines might be the result of a decrease in xylem area and/or the number of xylem vessels.

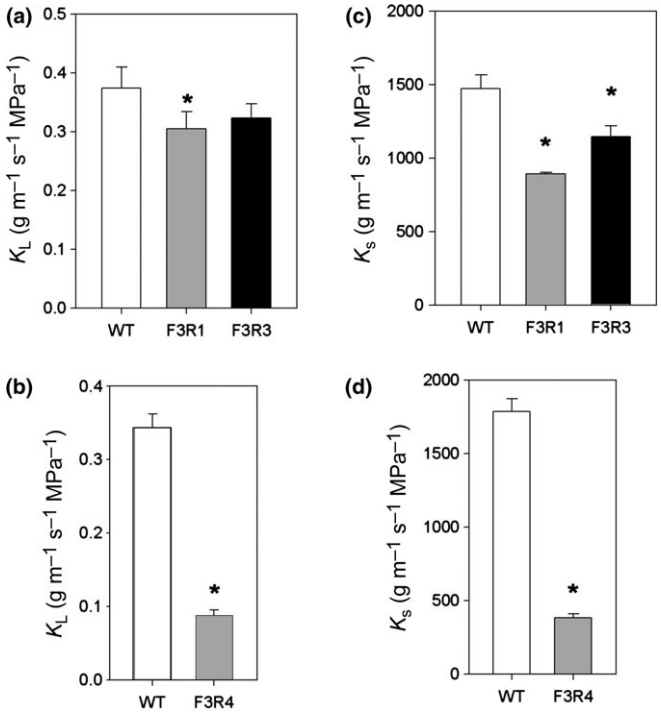

Fig. 5 *SlFRK3* suppression reduces tomato stem hydraulic conductivity. (a, b) Stem hydraulic conductivity normalized to xylem cross-sectional area (K_s). (c, d) Stem hydraulic conductivity normalized to leaf area (K_L). Data represent means (± SE) of five tomato (*Solanum lycopersicon*) plants. An asterisk denotes a significant difference ($P < 0.05$) between the mean stem hydraulic conductivity of a transgenic line and the wild-type (WT).

Significant reductions in root conductivity were also observed in all three lines. Root conductivity (Lr) calculated as the flow rate by pressure differences per root DW was reduced by 35%, 40% and 38% in F3R1, F3R3 and F3R4, respectively (relative to the WT; Fig. 6). Osmotically generated flow was also reduced in F3R1, F3R3 and F3R4. There were no significant differences in leaf hydraulic conductivity among the mature leaves (10th fully expanded leaf) of the WT, F3R1 and F3R3 plants (not shown). However, there was a significant loss in leaf hydraulic conductivity in the wilting mature leaves, but not the young leaves of F3R4, as compared with the WT (Fig. 7).

The wilting phenotype of F3R4 is due to a local effect in mature leaves

In order to determine whether the wilting phenotype of F3R4 was due to reduced water transport in the roots, stem or leaves, we performed two sets of grafting experiments. We performed a reciprocal grafting experiment with F3R4 and WT shoots and roots and also created double-grafted plants in which an F3R4 stem segment replaced a WT segment. Growth inhibition and the wilting phenotype of F3R4 were observed only when F3R4 was grafted as the shoot (Fig. 8). Because F3R4 roots and stems had no visible effect in the grafted plants, we suspected that the wilting phenotype and thin stems of F3R4 plants were due to reduced water transport in leaves.

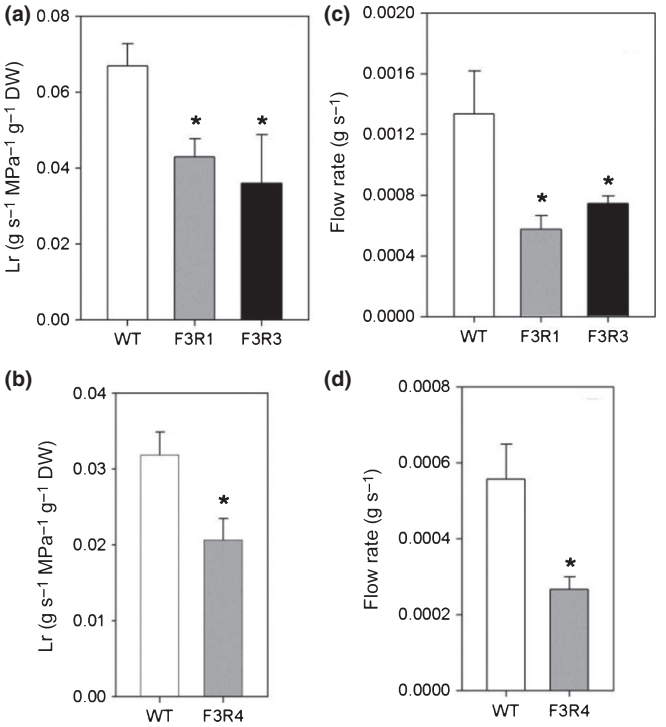

Fig. 6 *SlFRK3* suppression reduces tomato root hydraulic conductivity (Lr). Root conductivity (a, b) was determined based on pressure-driven exudation. (c, d) Root osmotically generated flow (no pressure applied). Data represent means (± SE) of six tomato (*Solanum lycopersicon*) plants. An asterisk denotes the presence of a significant difference ($P < 0.05$) between the mean root hydraulic conductivity of a transgenic line (F3R1, F3R3 or F3R4 plants) and the wild-type (WT).

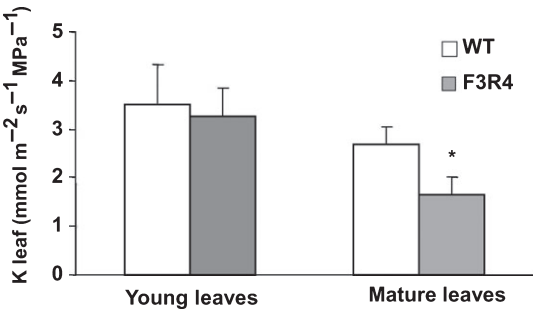

Fig. 7 Leaf hydraulic conductivity (K leaf). Data points represent the means (± SD) of eight tomato (*Solanum lycopersicon*) plants. A significant difference in hydraulic conductivity was observed in the mature leaves (10th fully expanded leaf) of F3R4 plants, but not in the young leaves (second fully expanded leaf) of F3R4 plants. Asterisk denotes a significant difference ($P < 0.05$) between the mean hydraulic conductivity of old wild-type (WT) leaves and old F3R4 leaves.

Cosuppression of *SlFRK3* and *SlFRK2* affects the development of secondary xylem fibers

In order to examine anatomical changes in leaves of F3R4 plants, we made cross-sections of petioles of young and mature leaves of F3R4 and WT plants. Cross-sections were also made of stems and stem–petiole junctions of mature leaves from these plants. Indeed, F3R4 petioles showed reduced lignification, resulting in parenchymatic regions (Fig. 9b) and dark necrotic tissue with collapsed cells (Fig. 9c,d). It seems that a dark secretion plugged the vessels and probably caused the wilting of mature leaves. The collapsed cells stimulated the formation of parenchyma around them (Fig. 9c,d). Remarkably, this phenotype was visible only in the vascular tissue of the leaf petiole and not in stems (Fig. S3f). A possible explanation for that is that this phenotype is caused by the cosuppression of *SlFRK3* and *SlFRK2* and that the level of *SlFRK2* suppression in F3R4 petioles is higher than that in stems (Fig. 2).

In order to check whether the altered phenotype of the F3R4 line is indeed caused by the suppression of both *SlFRK3* and *SlFRK2*, we crossed the F3R1 line (exhibiting specific suppression of *SlFRK3*) with the FRK2-antisense line (exhibiting specific suppression of *SlFRK2*; German *et al.*, 2003). The FRK2-antisense plants (Dai *et al.*, 2002; German *et al.*, 2003) and F3R1 plants exhibited no visible phenotypic alterations at the heterozygous state (F3R1 exhibited no visible phenotypic alteration even at the homozygous state, Fig. 3) and, accordingly, F_1 offspring of the F3R1xFRK2-antisense cross appeared normal. Among the F_2 segregating plants, only plants homozygous for FRK2-antisense and either homozygous or heterozygous for FRK3-RNAi exhibited similar severe growth inhibition and leaf wilting (Fig. 10). Extensive examination of the vascular tissues of five F_2 double-mutant plants exhibiting the severely altered phenotype revealed the presence of secondary xylem fibers with thin walls that occasionally collapsed (Fig. 11). When the thin-walled fibers collapsed, they usually did so in a wave pattern (large black arrows, Fig. 11b). This was followed by the production of parenchyma cells (P,

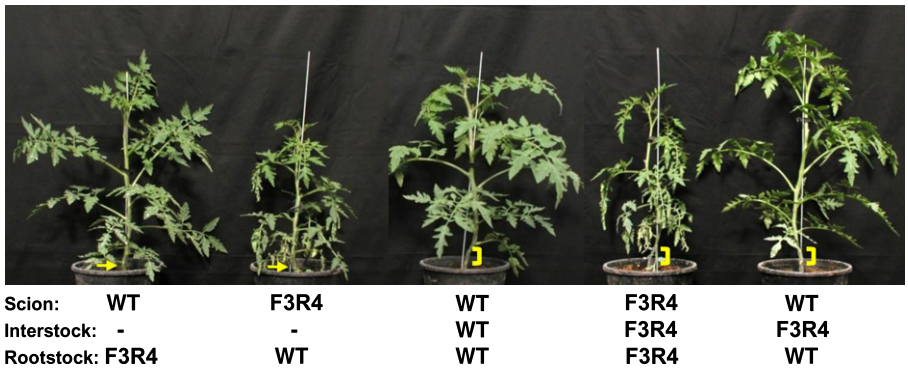

Fig. 8 Reciprocal and double grafting of F3R4 and wild-type (WT) tomato (*Solanum lycopersicon*) plants. Double grafts were performed in two consecutive steps (10 d apart) at the seedling stage. Plants were photographed *c*. 5 wk after the second grafting. The yellow arrows and brackets indicate the location of the reciprocal and double grafts, respectively.

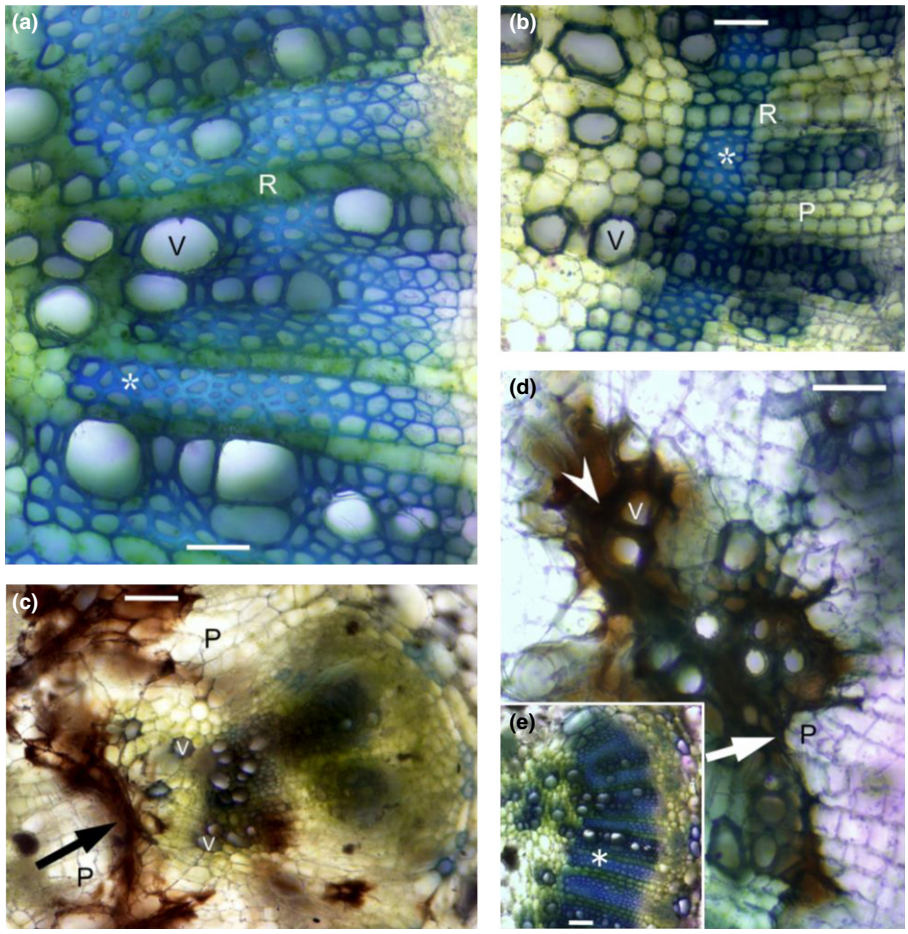

Fig. 9 Cross-sections of the F3R4 tomato (*Solanum lycopersicon*) leaf petiole at the stem–petiole junction. (a) Wild-type (WT) petiole. (b) F3R4 petiole with reduced fiber lignifications (the lignin is stained blue). (c, d) F3R4 petioles of older leaves (leaf no. 9) with dark necrotic tissue (arrowhead) with collapsed cells (arrows) around the vessels. (e) WT petiole control at the location shown in (c). The sections were stained with lacmoid. The necrotic lesions were also observed in fresh sections that had not been stained (Fig. S3). V, vessel; R, ray; P, parenchyma; *, secondary xylem fibers. Bars: (a, b, d) 50 μm; (c, e) 125 μm.

Fig. 11b). The thin-walled xylem fibers resulted in deformed xylem fibers (black arrowheads, Fig. 11c) being pressed between mature fibers (asterisk, Fig. 11c) and recently formed xylem parenchyma cells (P, Fig. 11c). We also observed xylem fibers whose differentiation was interrupted and whose partial cell walls (small arrows) did not form a continuous wall (Fig. 11d,e). In some fibers, we saw drops of a dark secretion outside the cells at the collapsed site (large white arrow, Fig. 11d) and inside the cells (small white arrows, Fig. 11d). These effects were not observed in FRK2-antisense plants; in those plants only xylem vessels were deformed (Fig. 11a). These results indicate that suppression of *SlFRK3* combined with suppression of *SlFRK2* interrupts xylem fiber development.

F3R4-distorted petioles reduce leaf sugar export

The damaged vascular tissue in the petioles of the mature leaves of the F3R4 plants seems to limit the flow of water into the leaves, leading to leaf wilting, but may also reduce the export of sugar from leaves, which may lead to low sugar levels in the stem. Indeed, analysis of the sugar content (sucrose, glucose and

Fig. 10 Cosuppression of *SlFRK3* and *SlFRK2* enhanced growth inhibition. Tomato (*Solanum lycopersicon*) plants were grown under normal conditions in the glasshouse and photographed *c*. 10 wk after germination. WT, wild-type.

fructose) of stem tissue and leaves revealed a reduction in the concentration of sugar in the stems of F3R4 plants, but not those of F3R1 and F3R3 plants (Fig. 12). Unlike the situation in the stem, the sugar contents of the leaves of F3R1, F3R3 and F3R4 lines were similar to those of control plants (Fig. 12), supporting the notion that the low levels of sugar observed in the stems of F3R4 plants are a result of the reduced transport of sugar out of the leaves.

Discussion

Expression pattern of *SlFRK3*

The present study illustrates the importance of *SlFRK3*, the only plastidic FRK found in tomato, for the development and functioning of the vascular tissue along with the major cytosolic fructose phosphorylating enzyme, *SlFRK2*. Using real-time PCR analysis, it has previously been shown that *SlFRK3* is expressed in all plant parts that have been examined (German *et al.*, 2004). However, the expression pattern in different tissues was not explored in that study. Promoter expression analysis in the current study revealed that *SlFRK3* is expressed in the vascular tissues of stems and leaves, in the cambium and differentiating xylem, in phloem companion cells and in young xylem fibers, suggesting that this gene plays a role in both xylem and phloem development. *SlFRK2* is also involved in vascular development (Damari-Weissler *et al.*, 2009). Although the GUS stain may be diffusible, no other types of cells were stained in the vicinity of the phloem companion cells and xylem fibers, suggesting that there was little to no diffusion from neighboring cells. The tissue-specific expression of *SlFRK2* has not yet been determined, yet its activity was found to be two to three times higher in secondary xylem than in the bark or pith of tomato stems (German *et al.*, 2003),

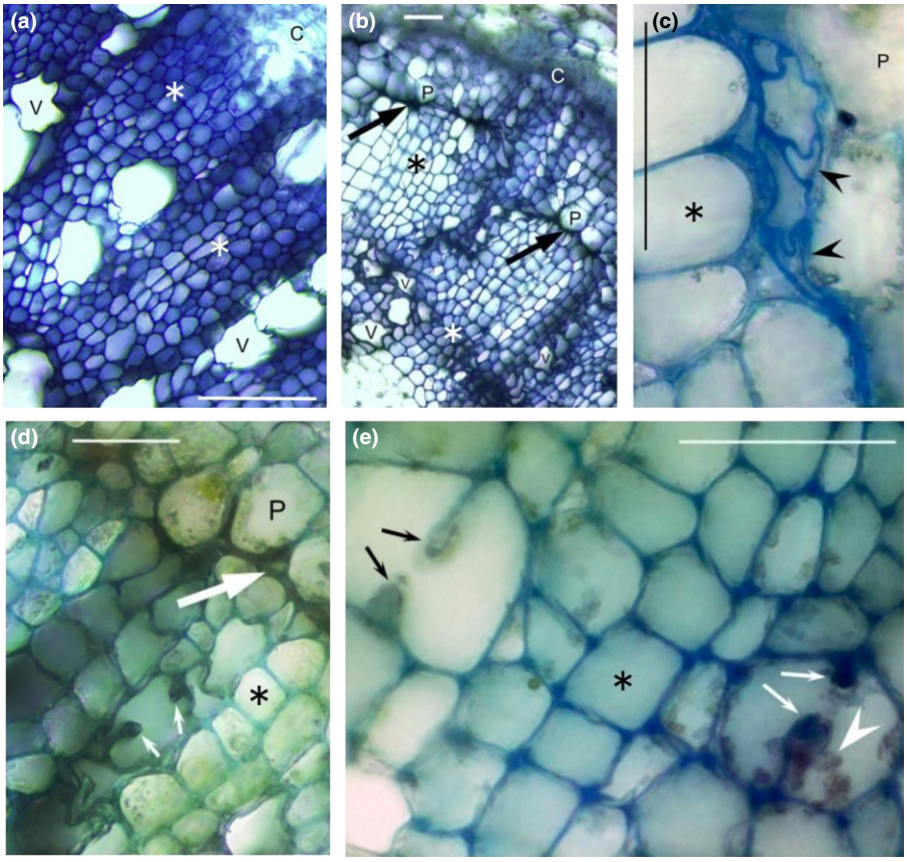

Fig. 11 Cosuppression of *SlFRK3* and *SlFRK2* affects secondary xylem fiber differentiation in stems of 6-wk-old tomato (*Solanum lycopersicon*) plants. (a) FRK2-antisense with deformed vessels (v) and normal fibers (*). (b) F3R3xFRK2 with typical front lines (large black arrows) of collapsed xylem fiber cells followed by parenchyma (P). (c) Thin-walled deformed xylem fibers (black arrowheads). (d, e) Dark secretions (large white arrowhead) inside differentiating xylem fibers that do not form complete cell walls (small arrows). The sections were stained with lacmoid. C, cambium. Bars, 50 μm.

indicating higher expression levels in vascular tissues. Therefore, it appears that both *SlFRK3* and *SlFRK2* are expressed primarily in vascular tissues, although it remains to be determined in which specific cell types *SlFRK2* is expressed and whether the two genes share common spatial and temporal expression patterns. The spatial expression patterns of *SlFRK3* (Fig. 1) and *SlFRK2* activity (German *et al.*, 2003) correlate with the expression of *SlSUS1*, the major sucrose synthase (SuSy) in tomato, which is also expressed mostly in vascular tissues (Goren *et al.*, 2011). Sucrose synthase cleaves sucrose into fructose and UDP-glucose, probably making fructose the most abundant nonphosphorylated hexose in the vascular tissue, underscoring the importance of FRKs for vascular development.

Role of *SlFRK3* in vascular development

Although only the F3R1 line exhibits specific *SlFRK3* suppression, the F3R3 line shares the same phenotype, with reduced hydraulic conductivity in stems and roots, but not in leaves, and moderate abortion of flowers, with an otherwise normal appearance. Because *SlFRK3* is the only *FRK* suppressed in both lines, we assume that the similar phenotype of these two lines is caused primarily by the suppression of *SlFRK3*.

Suppression of *SlFRK3* in the F3R1 and F3R3 lines slightly decreases the relative xylem area in the stem, perhaps by reducing cambial activity. This reduces the water conductivity of stem and roots and lowers the rate of transpiration (Figs 4–6). Anatomical analysis of F3R1 and F3R3 plants did not reveal any differences in the shape or size of the xylem vessels, as had been observed in *SlFRK2* antisense plants (Damari-Weissler *et al.*, 2009).

The third FRK3-RNAi line, F3R4, exhibited partial suppression of *SlFRK2* in addition to almost complete suppression of *SlFRK3*, and had unlignified, thin-walled secondary xylem fibers and dark necrotic areas in its petioles, but not its stems, perhaps due to higher cosuppression of *SlFRK2* in petioles as compared with stems (Fig. 2). As a result, the F3R4 line exhibits a unique phenotype of wilting mature leaves. Grafting experiments showed that F3R4 roots and stems had no effect on plant development or leaf wilting; whereas F3R4 shoots alone were sufficient to impose the phenotype of intact F3R4 plants, suggesting that the effect on leaf petioles is probably the major cause for this unique phenotype.

Although *SlFRK1* is also suppressed in F3R4 petioles, we believe that this suppression is not the cause of the phenotype, because *SlFRK1* is also suppressed in the F3R3 line and those plants exhibited normal growth. This conclusion is also supported by the double-transgenic plants formed by crossing the *SlFRK2*-antisense line and the F3R1 line that exhibited the F3R4 phenotype, supporting the notion that the combined suppression of *SlFRK3* and *SlFRK2* is sufficient to cause this phenotype. The double-transgenic plants exhibited severe growth inhibition, wilting of leaves, deformed thin cell walls of secondary xylem vessels and fibers, and dark necrotic areas with collapsed cells in the vascular tissue of their petioles and stems. The collapsed cells in these stems resembled the collapsed cells in the leaf petioles of F3R4, supporting the assumption that this phenotype is caused by the cosuppression of *SlFRK3* and *SlFRK2*. The severe phenotype of the double-transgenic plants (more than that of F3R4) shows that the combined near-complete suppression of *SlFRK3* and *SlFRK2* has an additive effect.

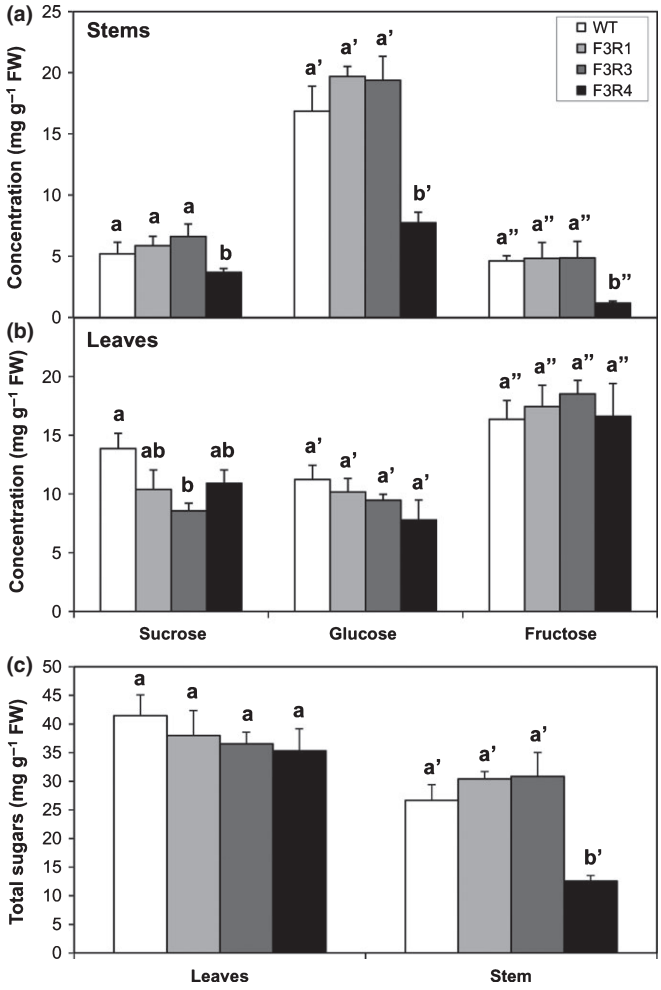

Fig. 12 Soluble sugars (sucrose, glucose and fructose) concentrations in the leaves and stems of the *SlFRK3*-RNAi transgenic tomato (*Solanum lycopersicon*) plants. (a) Sucrose, glucose and fructose in stems. (b) Sucrose, glucose and fructose in leaves. (c) Total sugars (sucrose + glucose + fructose) in stems and leaves of the *SlFRK3*-RNAi lines. Data are the means ± SE of six tomato plants. Different letters represent values that are significantly different within the same group (Student's *t*-test; $P < 0.05$). WT, wild-type.

It has been shown previously that *SlFRK2* is crucial for the proper development of cell walls of secondary xylem vessels and its suppression has been shown to lead to deformed thin-wall vessels (Damari-Weissler *et al.*, 2009). It was also reported that *SlFRK2* suppression reduced cambial activity and slowed the differentiation of secondary xylem fibers (Damari-Weissler *et al.*, 2009). Yet suppression of *SlFRK2* does not affect the shape of these fibers (Damari-Weissler *et al.*, 2009). In the current study, cosuppression of *SlFRK3* and *SlFRK2* caused the deformation and collapse of these fibers, indicating the importance of both cytosolic and the plastidic FRKs for secondary xylem fiber development.

Plastidic fructose metabolism and vascular development

The importance of *SlFRK2*, the main cytosolic FRK, for cell wall synthesis has previously been suggested (Damari-Weissler *et al.*, 2009), but the importance of *SlFRK3* for the cell wall is novel. The cytosolic FRK2 has been shown to be important for cellulose synthesis in aspen wood, in which the suppression of *FRK2* results in less cellulose and narrower xylem fibers (Roach *et al.*, 2012). The *SlFRK2* antisense phenotype of deformed xylem vessels in tomato plants resembles many of the Arabidopsis *irx*1-15 mutants that have defects in genes involved in cell wall synthesis and modification, such as cellulose synthase (Turner & Somerville, 1997; Brown *et al.*, 2005, 2007, 2011). It is easy to envision how FRK2, located in the cytosol, might contribute to the production of cytosolic UDP-Glc, the substrate of cellulose synthase located in the plasma membrane (Bowling & Brown, 2008), but it is less clear how FRK3 located in plastids might contribute to cell wall synthesis. Phosphorylation of fructose by the cytosolic FRK2 may alleviate fructose inhibition of SuSy, also located in the cytosol, thereby enhancing the cleavage of sucrose by SuSy, to yield UDP-Glc and fructose. Yet, there is no evidence that fructose phosphorylation within plastids alleviates fructose inhibition of SuSy.

Furthermore, the existence and source of fructose within plastids is not yet clear. Fructose is not produced in plastids through photosynthesis or through the degradation of starch, but could potentially be transported into plastids by hexose transporters (Schafer & Heber, 1977) or generated within plastids following cleavage of sucrose by invertase or SuSy. Although there have been reports of sucrose formation in isolated chloroplasts and invertase activity in plastids (Everson *et al.*, 1967; Vargas *et al.*, 2008), other efforts to detect sucrose, fructose and SuSy in chloroplasts have been unsuccessful (Albertsson & Larsson, 1976) and, to date, no plastidic sucrose transporter has been identified.

Once phosphorylated within plastids, the phosphorylated fructose may be subjected to plastidic glycolysis or fed into the pentose phosphate pathway or a starch synthesis pathway, although the absence of any effect on starch content in the FRK3-RNAi lines probably rules out the latter possibility (Fig. S4). The pentose phosphate pathway in plants is thought to have a strong effect on the flow of carbohydrates into the shikimic acid pathway to support the synthesis of aromatic amino acids (Maeda & Dudareva, 2012). Aromatic amino acids are essential for the synthesis of a large number of aromatic primary and secondary metabolites, such as auxin and lignin. Lignin biosynthesis depends on the supply of phenyl alanine from the plastids. The reduced lignification observed in the petioles of the F3R4 plants may indicate that *SlFRK3* is required for vascular lignification, which is necessary for cell wall hardiness, and may explain the cellular damage and deformation of fibers in the vascular tissues. An initial metabolite analysis suggested that F3R4 plants may have slightly lower levels of aromatic amino acids such as phenylalanine and tryptophan (Table S3), supporting the notion that *SlFRK3* may be important for the shikimic acid pathway, lignin biosynthesis and vascular lignification. However, significant reductions in the levels of other amino acids, such as alanine, threonine, aspartate, glutamate, aspargine and glutamine, as well as a reduction in total amino acid content (Table S3) suggest a wider effect on the production or transport of amino acids.

The phenotype of F3R4 and the F3R1xFRK2-antisense cross indicate an additive effect of *SlFRK3* and *SlFRK2* suppression, suggesting that the plastidic and cytosolic FRKs may compensate for each other to some degree. Although phosphorylated fructose cannot move into and out of plastids via a glucose-phosphate transporter (Kammerer *et al.*, 1998) and no fructose-phosphate transporter has been identified, phosphoglucose isomerase may convert F6P to G6P in both plastids and the cytosol. It is also possible that cytosolic and plastidic FRK partially compensate for each other through downstream metabolic pathways. Nevertheless, the developmental and phenotypic effects of *SlFRK3* suppression (manifested in lines F3R1 and F3R3 plants) are different from those observed in *SlFRK2*-antisense plants (Damari-Weissler *et al.*, 2009), suggesting that the plastidic FRK3 and the cytosolic FRK2 have unique functions also. On the one hand, suppression of *SlFRK2* inhibited growth and caused the wilting of young leaves, as well as produced deformed xylem vessels. Suppression of *SlFRK3*, on the other hand, had no effect on plant growth, but slightly affected xylem development, reduced hydraulic conductivity and caused abortion of flowers. In addition, combined suppression of both *SlFRK3* and *SlFRK2* distorted xylem fiber development. This study shows that *SlFRK2* and *SlFRK3* together are necessary for xylem fiber development and that the plastidic FRK3 is essential for proper xylem development and function.

Acknowledgements

We wish to thank Mr Leonid Mourakhovsky for his dedicated and diligent care of the tomato plants grown for this research. We also wish to thank Yael Hacham and Ifat Matityahu for technical assistance with the amino acid analysis. This research was supported by grant nos. IS-3897-06 and IS-4541-12 from BARD, the United States–Israel Binational Agricultural and Development Fund, and by research grant no. 890/06 from The Israel Science Foundation (ISF). Contribution from the Agriculture Research Organization, The Volcani Center, Bet Dagan, Israel, no. 120/2014 series.

Author contributions

O.S. and D.G. planned and designed the research and wrote the manuscript, O.S., H.D-W., F.S., S.R., Y.Y., R. Aloni and M.A.Z. performed experiments, M.A.G. made the RNAi construct, O.S., F.S., S.R., R. Aloni, A.S., N.M.H., R. Amir, M.A.Z. and D.G. analyzed the data.

References

Albertsson PA, Larsson C. 1976. Properties of chloroplasts isolated by phase partition. *Molecular and Cellular Biochemistry* **11**: 183–189.

Aloni R. 1980. Role of auxin and sucrose in the differentiation of sieve and tracheary elements in plant tissue cultures. *Planta* **150**: 255–263.

Barg R, Pilowsky M, Shabtai S, Carmi N, Szechtman AD, Dedicova B, Salts Y. 1997. The TYLCV-tolerant tomato line MP-1 is characterized by superior transformation competence. *Journal of Experimental Botany* **48**: 1919–1923.

Bowling AJ, Brown RM. 2008. The cytoplasmic domain of the cellulose-synthesizing complex in vascular plants. *Protoplasma* **233**: 115–127.

Brown D, Wightman R, Zhang Z, Gomez LD, Atanassov I, Bukowski JP, Tryfona T, McQueen-Mason SJ, Dupree P, Turner S. 2011. Arabidopsis genes IRREGULAR XYLEM (IRX15) and IRX15L encode DUF579-containing proteins that are essential for normal xylan deposition in the secondary cell wall. *Plant Journal* **66**: 401–413.

Brown DM, Goubet F, Wong VW, Goodacre R, Stephens E, Dupree P, Turner SR. 2007. Comparison of five xylan synthesis mutants reveals new insight into the mechanisms of xylan synthesis. *Plant Journal* **52**: 1154–1168.

Brown DM, Zeef LA, Ellis J, Goodacre R, Turner SR. 2005. Identification of novel genes in Arabidopsis involved in secondary cell wall formation using expression profiling and reverse genetics. *Plant Cell* **17**: 2281–2295.

Dai N, German MA, Matsevitz T, Hanael R, Swartzberg D, Yeselson Y, Petreikov M, Schaffer AA, Granot D. 2002. *LeFRK2*, the gene encoding the major fructokinase in tomato fruits, is not required for starch biosynthesis in developing fruits. *Plant Science* **162**: 423–430.

Damari-Weissler H, Kandel-Kfir M, Gidoni D, Mett A, Belausov E, Granot D. 2006. Evidence for intracellular spatial separation of hexokinases and fructokinases in tomato plants. *Planta* **224**: 1495–1502.

Damari-Weissler H, Rachamilevitch S, Aloni R, German MA, Cohen S, Zwieniecki MA, Michele Holbrook N, Granot D. 2009. *LeFRK2* is required for phloem and xylem differentiation and the transport of both sugar and water. *Planta* **230**: 795–805.

Dennis DT, Blakeley SD. 2000. Carbohydrate metabolism. In: Buchanan BB, Gruissem W, Jones RL, eds. *Biochemistry and molecular biology of plants*. Rockville, MD, USA: American Society of Plant Physiologists, 676–728.

Dinar M, Rudich J, Zamski E. 1983. Effects of heat-stress on carbon transport from tomato leaves. *Annals of Botany* **51**: 97–103.

Everson RG, Cockburn W, Gibbs M. 1967. Sucrose as a product of photosynthesis in isolated spinach chloroplasts. *Plant Physiology* **42**: 840–844.

German MA, Asher I, Petreikov M, Dai N, Schaffer AA, Granot D. 2004. Cloning, expression and characterization of *LeFRK3*, the fourth tomato (*Lycopersicon esculentum* Mill.) gene encoding fructokinase. *Plant Science* **166**: 285–291.

German MA, Dai N, Chmelnitsky I, Sobolev I, Salts Y, Barg R, Schaffer AA, Granot D. 2002. *LeFRK4*, a novel tomato (*Lycopersicon esculentum* Mill.) fructokinase specifically expressed in stamens. *Plant Science* **163**: 607–613.

German MA, Dai N, Matsevitz T, Hanael R, Petreikov M, Bernstein N, Ioffe M, Shahak Y, Schaffer AA, Granot D. 2003. Suppression of fructokinase encoded by *LeFRK2* in tomato stem inhibits growth and causes wilting of young leaves. *Plant Journal* **34**: 837–846.

Goren S, Huber SC, Granot D. 2011. Comparison of a novel tomato sucrose synthase, SlSUS4, with previously described SlSUS isoforms reveals distinct sequence features and differential expression patterns in association with stem maturation. *Planta* **233**: 1011–1023.

Gorska A, Ye Q, Holbrook NM, Zwieniecki MA. 2008. Nitrate control of root hydraulic properties in plants: translating local information to whole plant response. *Plant Physiology* **148**: 1159–1167.

Granot D. 2007. Role of tomato hexose kinases. *Functional Plant Biology* **34**: 564–570.

Kammerer B, Fischer K, Hilpert B, Schubert S, Gutensohn M, Weber A, Flugge UI. 1998. Molecular characterization of a carbon transporter in plastids from heterotrophic tissues: the glucose 6-phosphate/phosphate antiporter. *Plant Cell* **10**: 105–117.

Kanayama Y, Dai N, Granot D, Petreikov M, Schaffer A, Bennett AB. 1997. Divergent fructokinase genes are differentially expressed in tomato. *Plant Physiology* **113**: 1379–1384.

Kanayama Y, Granot D, Dai N, Petreikov M, Schaffer A, Powell A, Bennett AB. 1998. Tomato fructokinases exhibit differential expression and substrate regulation. *Plant Physiology* **117**: 85–90.

Kocacinar F, Sage RF. 2004. Photosynthetic pathway alters hydraulic structure and function in woody plants. *Oecologia* **139**: 214–223.

Maeda H, Dudareva N. 2012. The shikimate pathway and aromatic amino acid biosynthesis in plants. *Annual Review of Plant Biology* **63**: 73–105.

Petreikov M, Dai N, Granot D, Schaffer AA. 2001. Characterization of native and yeast-expressed tomato fruit fructokinase enzymes. *Phytochemistry* **58**: 841–847.

Renz A, Stitt M. 1993. Substrate-specificity and product inhibition of different forms of fructokinases and hexokinases in developing potato tubers. *Planta* **190**: 166–175.

Roach M, Gerber L, Sandquist D, Gorzsas A, Hedenstrom M, Kumar M, Steinhauser MC, Feil R, Daniel G, Stitt M *et al.* 2012. Fructokinase is required for carbon partitioning to cellulose in aspen wood. *Plant Journal* **70**: 967–977.

Schafer G, Heber U. 1977. Glucose transport into spinach chloroplasts. *Plant Physiology* **60**: 286–289.

Schaffer AA, Petreikov M. 1997. Sucrose-to-starch metabolism in tomato fruit undergoing transient starch accumulation. *Plant Physiology* **113**: 739–746.

Sinclair TR, Zwieniecki MA, Holbrook NM. 2008. Low leaf hydraulic conductance associated with drought tolerance in soybean. *Physiologia Plantarum* **132**: 446–451.

Turner SR, Somerville CR. 1997. Collapsed xylem phenotype of Arabidopsis identifies mutants deficient in cellulose deposition in the secondary cell wall. *Plant Cell* **9**: 689–701.

Vargas WA, Pontis HG, Salerno GL. 2008. New insights on sucrose metabolism: evidence for an active A/N-Inv in chloroplasts uncovers a novel component of the intracellular carbon trafficking. *Planta* **227**: 795–807.

Zwieniecki MA, Brodribb TJ, Holbrook NM. 2007. Hydraulic design of leaves: insights from rehydration kinetics. *Plant, Cell & Environment* **30**: 910–921.

Supporting Information

Additional supporting information may be found in the online version of this article.

Fig. S1 Alignment of an FRK3-RNAi fragment with the corresponding regions of *SlFRK1* and *SlFRK2*.

Fig. S2 Effect of *SlFRK3* suppression on relative xylem area.

Fig. S3 Cross-sections of petioles and petiole–stem junctions of F3R4 and WT plants.

Fig. S4 Starch content of leaves.

Table S1 Quantitative real-time PCR primers used in this study

Table S2 Mean stomatal aperture and density values

Table S3 Amino acid quantification in F3R4 and WT stems

Please note: Wiley Blackwell are not responsible for the content or functionality of any supporting information supplied by the authors. Any queries (other than missing material) should be directed to the *New Phytologist* Central Office.